*Optica Applicata, Vol. XLI, No. 1, 2011*

# Research on new spectral reconstruction solutions for Fourier-transform spectrometer

SUNING LI, RIHONG ZHU*, JIANXIN LI

Department of Optical Engineering, School of Electronic Information and Optical Engineering, Nanjing University of Science and Technology, Nanjing, Jiangsu Province, China

*Corresponding author: zhurihong@vip.sina.com

The spectral reconstruction of Fourier transform spectrometer can be simply achieved by using a Fourier transform or a Fourier cosine transform. However, the traditional Fourier transform solution is carried out in the complex-number field and the result is also a complex-number sequence, which will introduce an extra-phase to the spectrum and lead to the inaccuracy of reconstructed spectral intensity. On the other hand, although researchers use a Fourier cosine transform to avoid the extra-phase problem effectively, this solution has a boundary condition problem which cannot be avoided and may also lead to the inaccuracy of the reconstructed spectral intensity. To solve the problem, an improved Hilbert transform reconstruction solution (IHTRS) and a Fourier conjugated correction reconstruction solution (FCCRS) are developed by analyzing traditional reconstruction solutions. The main thought of IHTRS is using a complex-number sequence to represent the real-number signal, doing the transform in the complex-number field, and extracting the real-number spectrum from the transform result in the end. The main thought of FCCRS is constraining the transform process in the real-number field, using the conjugated property of the Fourier transform, creating the conjugated symmetrical form of the original signal first and acquiring the conjugated symmetrical form of the real spectrum, and extracting the real spectrum from it in the end. The results of the two solutions are compared. By carrying out both the simulation and the experiment using a helium lamp, it can be concluded that the FCCRS is 3 times faster than IHTRS, while the reconstructed spectral intensity accuracy of IHTRS is 29% higher than FCCRS. Both of the two solutions can avoid either the extra-phase problem caused by a discrete Fourier transform (DFT) solution or the boundary condition caused by a discrete cosine transform (DCT) solution effectively and improve the reconstructed spectral intensity accuracy.

Keywords: imaging spectroscopy, reconstruction, spectrum, Fourier transform, Hilbert transform, conjugated correction.

## 1. Introduction

Since the Fourier transform was firstly used in getting the spectrum of a light source by LOEWENSTEIN in 1966 [1], the Fourier transform spectroscopy has been developed [2–4]. With the Fellgett advantage (or multiplex advantage), the Jacquinot

advantage (or throughput advantage) [5] and the high SNR advantage [6], the Fourier transform spectrometer is widely used today, for instance in the remote sensing field, chemical industry, THz field which has been developed in recent years, *etc*. [2, 7–9]. And by the use of the Fourier transform spectroscopy, it becomes possible to improve remarkably the measurement accuracy as well as the efficiency with a more compact and stable structure [2, 4, 10, 11].

The spectral reconstruction solution of the Fourier-transform spectrometer is mainly based on the Fourier transform relationship between the spectrum and the interferogram of a light source [12]. Traditionally, the reconstructed spectrum is the real part or the absolute magnitude of the Fourier transform result which is a complex number [12, 13]. That is to say, the reconstruction process brings in an extra-phase information which actually does not exist in spectral information. Therefore, the prerequisite that the spectrum should exactly be reconstructed in the real field will not be satisfied and there will certainly be errors in the reconstruction process. As a result, the Fourier cosine transform, the expressive form of the Fourier transform in the real number field, has been used as a spectral reconstruction method [14, 15]. However, because of a real-even symmetric transform, with different boundary conditions, the results are also different, which leads to the inaccurately reconstructed spectrum [16–20]. To solve this problem, in the second part, the traditional spectral reconstruction solutions are analyzed, in the third part, the IHTRS is developed and discussed, in the fourth part, the FCCRS is developed and discussed. The simulations and the helium lamp spectral reconstruction experiments are carried out, the results of traditional solutions and the two new developed solutions are compared with each other in the fifth part. The discussion is provided in the sixth part.

## 2. Theory of traditional spectral reconstruction

The Fourier transform spectroscopy is simply based on the Fourier-transform pairs relationship between the spectrum and the corresponding interferogram.

The spectrum reconstructed from an error-free interferogram can be expressed as

$$B(\sigma) = 2\int_0^{\infty} I(\Delta)\cos(2\pi\sigma\Delta)\mathrm{d}\Delta \tag{1}$$

where $B(\sigma)$ is the spectrum reconstructed and $I(x)$ is the interferogram captured by the spectrometer, $\sigma$ denotes the wave number, $\Delta$ is the optical path difference (OPD).

Assuming $B(\sigma)$ is an even-function, that is, $B(-\sigma) = B(\sigma)$, and expanding the range of $\sigma$ to $-\infty \sim +\infty$, it can be concluded from Eq. (1) that

$$I(\Delta) = 2\int_0^{+\infty} B(\sigma)\cos(2\pi\sigma\Delta)\mathrm{d}\sigma = \int_{-\infty}^{+\infty} B(\sigma)\exp(j2\pi\sigma\Delta)\mathrm{d}\sigma \tag{2}$$

Equation (2) shows that the interferogram $I(\Delta)$ is the Fourier transform of $B(\sigma)$ which is an even-function. To be simple, the relationship between the interferogram and the source spectrum can be expressed as the Fourier-transform pairs below

$$I(\Delta) = \mathrm{FT}\left[B(\sigma)\right] \tag{3}$$

$$B(\sigma) = \mathrm{FT}^{-1}\left[I(\Delta)\right] \tag{4}$$

where $I(\Delta)$ is also assumed to be an even-function and the range of $\Delta$ is expanded to $-\infty \sim +\infty$. Considering that the interferogram is captured in a discrete way by a computer, the equations above should be written in a discrete form

$$I(\Delta) = \mathrm{DFT}\left[B(\sigma)\right] \tag{5}$$

$$B(\sigma) = \mathrm{IDFT}\left[I(\Delta)\right] \tag{6}$$

where DFT denotes the discrete Fourier transform and IDFT is the inverse discrete Fourier transform.

The conventional spectrum reconstruction solution is based on the relationship expressed by Eqs. (5) and (6). The problem is, as the kernel of the Fourier transform is a complex number, that the result of the reconstruction will also be a complex number, which downright falls short of the real-number format of the real spectrum. Mostly, to fix the issue, people simply use the real part or the absolute magnitude of the transformation result as the reconstructed spectrum [12, 13]. However, this solution will bring in the extra-phase information and may lead to errors of the reconstructed spectral intensity, and more, according to the physical definition, $\sigma$ is always a positive value so that there is not any value suitable for $B(\sigma)$ when $\sigma$ is negative.

To resolve this issue, researchers developed a new spectral reconstructed solution using the Fourier cosine transform which is the real-field expression of the Fourier transform and can constrain the reconstruction in the real-number field to avoid the extra-phase-information problem [14–20]. In the engineering concept, the discrete cosine transform (DCT) is real and orthogonal, with a real-number transform kernel. There have already been 16 kinds of DCT forms through years of development, and the widest used one is DCT-II [21, 22] as

$$B(k) = \left(\frac{2}{N}\right)^{1/2} c_k \sum_{n=0}^{N-1} I(n) \cos\left[\frac{(2n+1)k\pi}{2N}\right], \quad k = 0, 1, ..., N-1 \tag{7}$$

$$I(n) = \left(\frac{2}{N}\right)^{1/2} \sum_{k=0}^{N-1} c_k B(k) \cos\left[\frac{(2n+1)k\pi}{2N}\right], \quad n = 0, 1, ..., N-1 \tag{8}$$

where

$$c_k = \begin{cases} \dfrac{1}{\sqrt{2}}, & k = 0, N \\ 1 & k = 1, 2, \ldots, N-1 \end{cases} \tag{9}$$

According to the definition, DCT can be considered as the DFT of a real-even sequence with all the imaginary-sine parts balanced out and all the real-cosine parts reserved. Whereas, supposing there is a discrete sequence $I(n)$ ($n = 0, 1, ..., N-1$) with the length $N$, the symmetrical sequence $I_s(k)$ with the length $N_s$ is created from $I(n)$, which satisfies the equation $I_s(k) = I_s(N_s - 1 - k)$ ($k = 0, 1, ..., N-1$). It can be found that there exist two different kinds of symmetry of $I_s(k)$ with different values of $N_s$ as $N_s = 2N - 1$ or $N_s = 2N$, which will lead to different reconstructed results after carrying out DFT towards $I_s(k)$. On the other hand, compared with the definition of DCT, it can be concluded that the two different results are also different from the result of using DCT directly to the original sequence $I(n)$. Considering the properties of cosine function, the error raised by the boundary condition of DCT can also be treated as an extra-phase like that in DFT solution. Consequently, the result of the DCT solution for spectral reconstruction is also inaccurate though it can avoid some of the impact by the extra-phase problem.

## 3. Improved Hilbert transform reconstruction solution

It can be concluded from the above paragraphs that, no matter whether the transfer kernel is complex or not, both the DFT and the DCT solution will bring in an extra--phase. If we actively bring an extra-phase in the interferogram and make the spectral reconstruction be carried out in the complex field, and use it to balance out the spectral extra-phase caused by the transform itself, the problem can be solved. In other words, we can create a virtual complex signal from the real signal and thus reconstruct the spectrum by which instead of reconstructing the spectrum from the original real signal.

Let $B_r(\sigma)$ be the spectrum of the interferogram $I_r(x)$ which is a real-number signal. Define a complex-number signal $I_c(x)$, which satisfies the equation

$$I_c(x) = \int_0^{\infty} 2B_r(\sigma)\cos(j2\pi\sigma x)\mathrm{d}\sigma \tag{10}$$

It can be found easily that the real part of $I_c(x)$ is the original signal $I_r(x)$. Define $B_c(\sigma)$ as the spectrum of $I_c(x)$, it can be concluded from Eq. (10) that

$$B_c(\sigma) = \begin{cases} 2B_r(\sigma), & \sigma > 0 \\ 0, & \sigma < 0 \end{cases} \tag{11}$$

When $\sigma = 0$, it is equivalent to the situation that there is a constant term in signal space, which corresponds to the situation that there is a $\delta$ function at $\sigma = 0$ in spectrum space. Therefore, $B_c(\sigma)$ can be written as

$$B_c(\sigma) = \begin{cases} 2B_r(\sigma), & \sigma > 0 \\ B_r(\sigma), & \sigma = 0 \\ 0, & \sigma < 0 \end{cases} \tag{12}$$

or

$$B_c(\sigma) = \left[1 + \operatorname{sgn}(\sigma)\right] B_r(\sigma) \tag{13}$$

where

$$\operatorname{sgn}(\sigma) = \begin{cases} 1, & \sigma > 0 \\ 0, & \sigma = 0 \\ -1, & \sigma < 0 \end{cases} \tag{14}$$

By carrying out the invert Fourier transform to Eq. (13), $I_c(x)$ can be expressed as

$$I_c(x) = I_r(x) + F^{-1}\{\operatorname{sgn}(\sigma)\} F^{-1}\{B_r(\sigma)\} =$$

$$= I_r(x) + \frac{j}{\pi x} I_r(x) = I_r(x) - \frac{j}{\pi} \int_{-\infty}^{+\infty} \frac{I_r(\alpha)}{\alpha - x} \mathrm{d}\alpha \tag{15}$$

where

$$\frac{1}{\pi} \int_{-\infty}^{+\infty} \frac{I_r(\alpha)}{\alpha - x} \mathrm{d}\alpha = \frac{1}{\pi} \lim_{\varepsilon \to 0} \left\{ \int_{-\infty}^{t-\varepsilon} \frac{I_r(\alpha)}{\alpha - x} \mathrm{d}\alpha + \int_{t+\varepsilon}^{+\infty} \frac{I_r(\alpha)}{\alpha - x} \mathrm{d}\alpha \right\} \tag{16}$$

Equation (16) is the Hilbert transform of $I_r(x)$. Thus, it can be concluded that the real part of $I_c(x)$ is equal to $I_r(x)$ and the imaginary part of $I_c(x)$ is equal to the Hilbert transform of $I_r(x)$.

Inverting all the steps above, we reach a solution for spectral reconstruction in the complex-number field. First, capture the interferogram $I_r(x)$ by the spectrometer; second, create the virtual interferogram $I_c(x)$ with $I_r(x)$ as its real part and the Hilbert transform of $I_r(x)$ as its imaginary part, that is

$$I_c(x) = I_r(x) - jH\{I_r(x)\} \tag{17}$$

where $H\{...\}$ denotes the Hilbert transform.

Third, by carrying out the Fourier transform to $I_c(x)$, the virtual spectrum $B_c(\sigma)$ can be acquired, and the real spectrum $B_r(\sigma)$ can then be acquired from $B_c(\sigma)$, according to Eq. (12).

## 4. Fourier conjugated correction reconstruction solution

From the paragraph above, it can be found that the results of IHTRS correspond to the definition of spectrum mathematically. However, the solution will take lots of steps to calculate and will cost a lot of time. By constraining the reconstruction process to the real-number field, instead of changing over between the complex-number and the real-number field, the reconstruction of the spectrum would be faster.

Considering the conjugated property of the Fourier transform and assuming a conjugated symmetric sequence, $I_s(n)$ satisfies

$$\begin{cases} I_s(N-n) = I_s^*(n), & n = 1, 2, \ldots, \dfrac{N}{2} - 1 \\ I_s(0) \text{ and } I_s\left(\dfrac{N}{2}\right) & \text{are real numbers} \end{cases} \tag{18}$$

The DFT of $I_s(n)$ is

$$B_s(k) = \sum_{n=0}^{N-1} I_s(n) W_N^{kn}, \quad k = 0, 1, \ldots, N-1 \tag{19}$$

where $W_N = \exp(-j2\pi/N)$, divide $B_s(k)$ into two parts as

$$B_s(k) = \sum_{n=0}^{N/2} I_s(n) W_N^{kn} + \sum_{n=\frac{N}{2}+1}^{N-1} I_s(n) W_N^{kn} \tag{20}$$

with the substitution of the upper and the lower limits of the summation, the equation can be written as

$$B_s(k) = \sum_{n=0}^{\frac{N}{2}} I_s(n) W_N^{kn} + \sum_{n=1}^{\frac{N}{2}-1} I_s(N-n) W_N^{k(N-n)} \tag{21}$$

As $I_s(n)$ and $W_N^{kn}$ are all conjugated and symmetric sequences which satisfy $I_s(N-n) = I_s^*(n)$, $W_N^{k(N-n)} = (W_N^{kn})^*$ and according to Eq. (21),

$$B_s(k) = \sum_{n=0}^{\frac{N}{2}} I_s(n) W_N^{kn} + \sum_{n=1}^{\frac{N}{2}-1} I_s^*(n) (W_N^{kn})^* \tag{22}$$

Expressing $I_s(n)$ in a complex way: $I_s(n) = I_{sr}(n) + jI_{si}(n)$ for $W_N^{kn} = \cos\left(\frac{2\pi}{N}kn\right) - j\sin\left(\frac{2\pi}{N}kn\right)$, then we can conclude from Eq. (22) that

$$B_s(k) = I_s(0)W_N^{k-0} + I_s\left(\frac{N}{2}\right)W_N^{k(N/2)} + \sum_{n=1}^{\frac{N}{2}-1}\left[I_s(n)W_N^{kn} + I_s^*(n)\,(W_N^{kn})^*\right] =$$

$$= I_s(0) + I_s\left(\frac{N}{2}\right)\cos(k\pi) + 2\sum_{n=1}^{\frac{N}{2}-1}\left[I_{sr}(n)\cos\left(\frac{2\pi}{N}kn\right) + I_{si}(n)\sin\left(\frac{2\pi}{N}kn\right)\right] \tag{23}$$

$k = 0, 1, ..., N-1$

In the same way, for the conjugated symmetric sequence $B_s(k)$ with $N$ points

$$I_s(n) = \frac{1}{N}B_s(0) + \frac{1}{N}B_s\left(\frac{N}{2}\right)\cos(n\pi) +$$

$$+ \frac{1}{N}\sum_{k=\frac{N}{2}-1}^{1}\left[B_s(k)W_N^{kn} + B_s^*(k)\,(W_N^{kn})^*\right] =$$

$$= \frac{1}{N}B_s(0) + \frac{1}{N}B_s\left(\frac{N}{2}\right)\cos(n\pi) +$$

$$+ \frac{2}{N}\sum_{k=1}^{\frac{N}{2}-1}\left[B_{sr}(k)\cos\left(\frac{2\pi}{N}kn\right) - B_{si}(k)\sin\left(\frac{2\pi}{N}kn\right)\right] \tag{24}$$

$n = 0, 1, ..., N-1$

It can be concluded from Eqs. (23) and (24), which are the DFT and IDFT of the conjugated symmetric sequence, that the result of the transform is related to the first and the middle element of the sequence – one is a constant value and the other is a fluctuating sequence. It can be assumed that the sequence with the two influencing elements removed is the real spectrum data as it contains the pure spectral information. In conclusion, let $I(n)$ be the interferogram captured and $I_s(k)$ be the sequence which has been made conjugated symmetric from $I(n)$, where $N$ is the number of sampling points, $n = 0, 1, ..., N-1$, $k = 0, 1, ..., 2N-1$, then

$$B_s(k) = \mathrm{IDFT}\left(I_s(k)\right) - \frac{1}{2N}I_s(0) - \frac{1}{2N}I_s(N)\cos(k\pi) \tag{25}$$

The spectral data $B_s(k)$ here is also a conjugated symmetric sequence. The single sided form of $B_s(k)$ is the real spectrum $B(n)$, $n = 0, 1, ..., N - 1$.

The paragraph above shows that FCCRS can avoid the boundary condition problem caused by DCT solution and the complex-number problem or the extra-phase problem caused by traditional DFT solution. In addition, when we compare Eq. (7) with Eq. (23), it can be acknowledged that, being different from DCT solution, the result of FCCRS is calculated from the interferogram without the first element. Second, it is impossible for DCT solution to remove the impact caused by the $N/2 + 1$ element of the conjugated symmetric sequence, which brings in the main error of the reconstruction result.

## 5. Simulation and experiment

To prove the correction of IHTRS and FCCRS, the simulation and the experiment are carried out. In order to compare the reconstructed accuracy, all the intensities of spectral results are relative.

The simulating steps are as follows:

1. Create the spectrum sequence stochastically with the computer program which we developed.

2. Create the interferogram by carrying out the Fourier transform of the simulated spectrum; considering the actual usage, the interferogram created is unilateral.

3. Reconstruct the spectrum from the interferogram with both the traditional DFT solution and DCT solution, IHTRS and FCCRS, and analyze the result.

Figures 1–3 are the results of the simulation. Figure 1 is the simulated spectrum created by the computer, Fig. 2 is the simulated interferogram created from the setting spectrum, and Fig. 3 shows the results of all four solutions, as well as the original spectrum for comparing. For more details, the zoomed out figure is provided at the top-left corner.

By comparing with the original spectrum, it is shown in Fig. 3 that there are spectral intensity errors of the spectrum reconstructed with traditional DFT and DCT solutions, especially in high frequency fields. The IHTRS and FCCRS are more

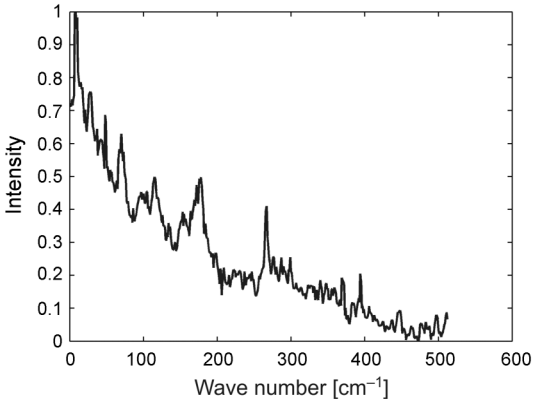


Fig. 1. Simulated spectrum.

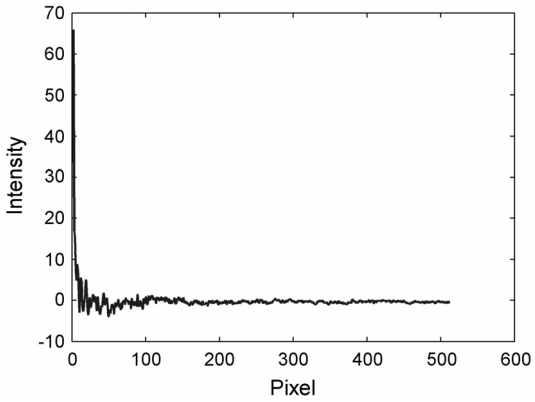


Fig. 2. Simulated interferogram.

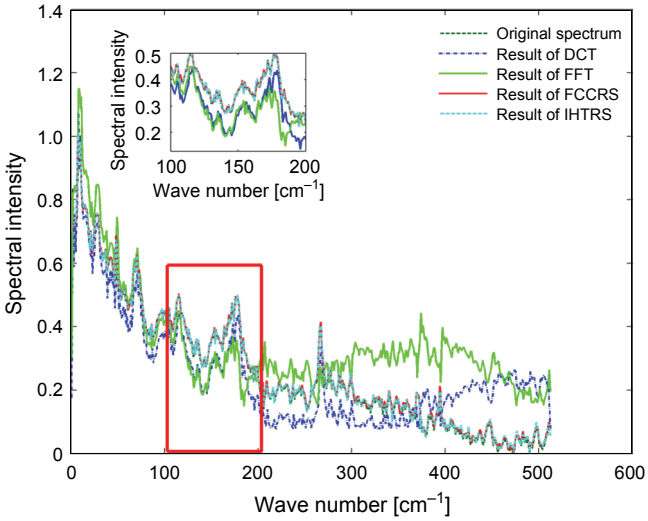


Fig. 3. Reconstructed simulated spectrum by different solutions.

effective, the results of which can fix the original spectrum well. The reconstructed error of each solution is evaluated by using the RMS value of the deviation between the reconstructed spectrum and the original spectrum, as shown in the Table.

With the use of a helium lamp, the experiment leading to the real source spectral reconstruction is carried out. Figure 4 is the interferogram captured by the Fourier transform imaging spectrometer developed by us. The standard spectrum is captured by a UV–IR dispersion spectrometer. The result is shown in Fig. 5. As the recon-

T a b l e. Reconstructed errors of each solution.

| | FFT | DCT | FCCRS | IHTRS |
|---|---|---|---|---|
| Simulated spectrum | 0.1217 | 0.1067 | 0.0103 | 0.0077 |
| Helium lamp spectrum | 0.0634 | 0.0614 | 0.0101 | 0.0071 |

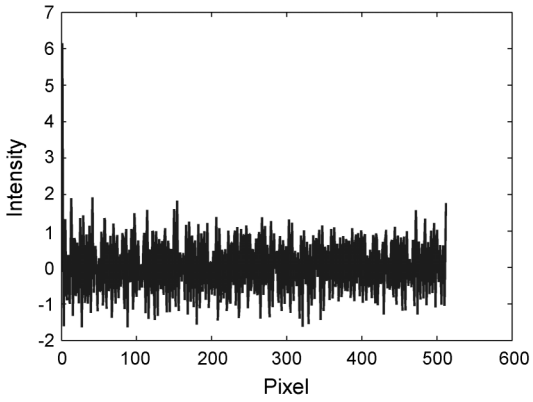


Fig. 4. Interferogram of helium lamp captured by Fourier transform spectrometer.

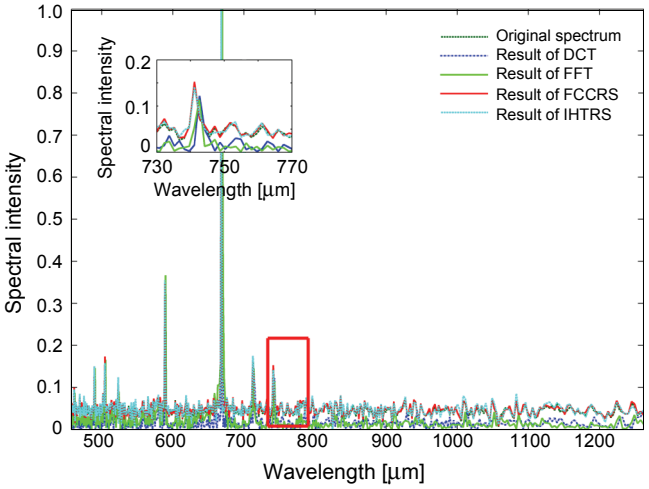


Fig. 5. Reconstructed spectrum of helium lamp by different solutions.

structed spectrum by IHTRS and FCCRS is close to the standard spectrum, their comparison is shown in Fig. 6. It can be concluded that all reconstructed solutions have a good accuracy in both reconstructed spectral intensity and frequency. With the use of FCCRS or IHTRS, the spectral intensity of the reconstructed spectrum can fix the standard spectrum better. Using the RMS value defined above to evaluate the reconstructed error, the data is also shown in the Table.

## 6. Discussion

Through the simulation and the helium lamp experiment, it can be concluded that both IHTRS and FCCRS have higher reconstructed spectral intensity accuracy than

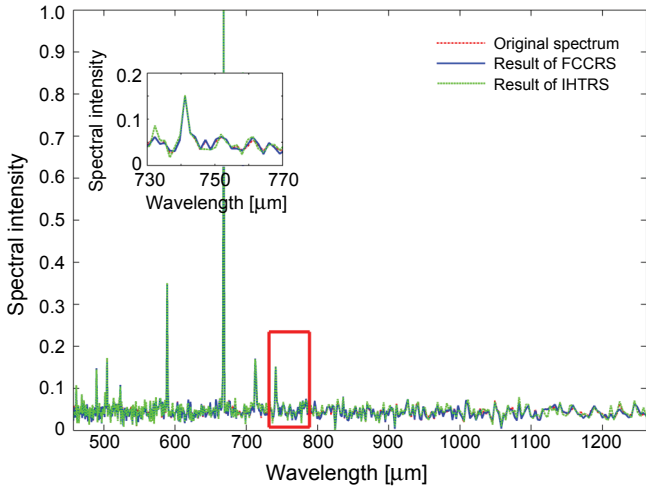


Fig. 6. Comparison of IHTRS and FCCRS.

traditional DFT and DCT solutions. But as IHTRS is calculated by transferring both in the real and complex number field, this process will make the solution cost much more time than DFT, DCT and FCCRS. FCCRS uses FFT solely in the real-number field, so it is as fast as DFT solution, and costs only 1/3 of the IHTRS time. But as FCCRS needs to remove the impact of the correction elements, some of the spectral information is also removed, while IHTRS agrees with the definition of spectrum mathematically. Thus, the reconstructed spectral intensity by IHTRS is more accurate than that of FCCRS, as shown in the Table.

## 7. Conclusions

To solve the extra-phase problem of the traditional DFT solution and the boundary--condition problem of the DCT solution, which has been widely used these years in spectral reconstruction of the Fourier transform spectrometer, IHTRS and FCCRS are presented and developed. With the simulation, it can be concluded that by using FCCRS, the reconstructed spectral intensity error can be reduced by 11.14%, compared with that by DFT solution and by 9.64%, compared with the result by DCT solution. By using IHTRS, the reconstructed spectral intensity error can be reduced by 11.4%, compared with that by DFT solution and by 9.9%, compared with the result by DCT solution. With the helium lamp experiment, it can be concluded that by using FCCRS, the reconstructed spectral intensity error can be reduced by 5.3%, compared with that by DFT solution and by 5.13%, compared with the result by DCT solution. By using IHTRS, the reconstructed spectral intensity error can be reduced by 5.63%, compared with that by DFT solution and by 5.43%, compared with the result by DCT solution.

Both FCCRS and IHTRS can constrain the reconstructed spectral intensity error in 1%, compared with the standard spectrum. FCCRS is 3 times faster than IHTRS, but the reconstructed spectral intensity error of IHTRS is 30% less than FCCRS. Both solutions have their own advantages and can be used according to the needs.

## References


[1] LOEWENSTEIN E.V., *The history and current status of fourier transform spectroscopy*, Applied Optics **5**(5), 1966, pp. 845–854.

[2] THURMAN S.T., FIENUP J.R., *Fizeau Fourier transform imaging spectroscopy: Missing data reconstruction*, Optics Express **16**(9), 2008, pp. 6631–6645.

[3] SELLAR R.G., RAFERT J.B., *Fourier-transform imaging spectrometer with a single toroidal optic*, Applied Optics **34**(16), 1995, pp. 2931–2933.

[4] KAWATA S., MINAMI K., MINAMI S., *Superresolution of Fourier transform spectroscopy data by the maximum entropy method*, Applied Optics **22**(22), 1983, pp. 3593–3598.

[5] LUC P., GERSTENKORN S., *Fourier transform spectroscopy in the visible and ultraviolet range*, Applied Optics **17**(9), 1978, pp. 1327–1331.

[6] TENG Y.C., RAYCE B.S.H., *Quantitative Fourier transform IR photoacoustic spectroscopy of condensed phases*, Applied Optics **21**(1), 1982, pp. 77–80.

[7] ALEKSEYEV L., NARIMANOV E., KHURGIN J., *Super-resolution imaging using spatial Fourier transform infrared spectroscopy*, Conference on Lasers and Electro-Optics 2009, Maryland, Baltimore, May 31, 2009, Nanophotonics and Metamaterial Symposium I, p. JWC5.

[8] THÉBERGE F., CHÂTEAUNEUF M., DUBOIS J., DÉSILETS S., LUSSIER L.-S., *Spectral artifacts from non-uniform samples analyzed by terahertz time-domain spectroscopy*, Optics Express **17**(13), 2009, pp. 10841–10848.

[9] DUPUIS J.R., ÜNLÜ M.S., *Time-domain surface profile imaging via a hyperspectral Fourier transform spectrometer*, Optics Letters **33**(12), 2008, pp. 1368–1370.

[10] ZHAO P., MARIOTTI J. -M., DU FORESTO V.C., LÉNA P., *Infrared single-mode fiber-optic Fourier--transform spectrometry and double Fourier interferometry*, Applied Optics **35**(16), 1996, pp. 2897–2901.

[11] PISANI M., ZUCCO M.E., *Compact imaging spectrometer combining Fourier transform spectroscopy with a Fabry–Perot interferometer*, Optics Express **17**(10), 2009, pp. 8319–8331.

[12] ESKOLA S.M., STENMAN F., *Interpolation of spectral data using shift theorem of the discrete Fourier transform*, Applied Spectroscopy **51**(8), 1997, pp. 1179–1184.

[13] HEINTZMANN R., LIDKE K.A., JOVIN T.M., *Double-pass Fourier transform imaging spectroscopy*, Optics Express **12**(5), 2004, pp. 753–763.

[14] POGRIBNY W., DRECHNY M., *Discrete cosine transform using modified DPCM*, Proceedings of SPIE **5484**, 2004, pp. 653–658.

[15] CASASENT D., PSALTIS D., *Optical Fourier transform techniques for advanced Fourier spectroscopy systems*, Applied Optics **19**(12), 1980, pp. 2034–2037.

[16] CHUJUN ZHENG, PENG HAN, HONGSEN CHANG, *Four-quadrant spatial phase-shifting Fourier transform digital holography for recording of cosine transform coefficients*, Chinese Optics Letters **4**(3), 2006, pp. 145–147.

[17] RUCKMONGATHAN T.N., *Discrete cosine transform for driving liquid crystal displays*, Journal of Display Technology **5**(7), 2009, pp. 243–249.

[18] SHERLOCK B.G., KAKAD Y.P., SHUKLA A., *Rapid update of odd DCT and DST for real-time signal processing*, Proceedings of SPIE **5809**, 2005, pp. 464–471.

[19] REEVES R., *New shift, scaling and derivative properties for the DCT*, Proceedings of SPIE **3653**, 1999, pp. 418–428.

[20] BALAM S.C., SCHONFELD D., *New algorithm for computation of DCT through pyramidal addition*, Proceedings of SPIE **5683**, 2005, pp. 208–217.

[21] YINGSONG HU, JIANGTAO XI, CHICHARO J., ENBANG LI, ZONGKAI YANG, *Discrete cosine transform--based shift estimation for fringe pattern profilometry using a generalized analysis model*, Applied Optics **45**(25), 2006, pp. 6560–6567.

[22] GHOLAM-ALI HOSSEIN-ZADEH, HAMID SOLTANIAN-ZADEH, *DCT acquisition and reconstruction of MRI*, Proceedings of SPIE **3338**, 1998, pp. 398–407.

*Received August 31, 2010*